

RESEARCH

Open Access



# Gait-based age estimation using multi-stage convolutional neural network

Atsuya Sakata<sup>1\*†</sup>, Noriko Takemura<sup>2†</sup> and Yasushi Yagi<sup>1</sup>

## Abstract

Gait-based age estimation has been extensively studied for various applications because of its high practicality. In this paper, we propose a gait-based age estimation method using convolutional neural networks (CNNs). Because gait features vary depending on a subject's attributes, i.e., gender and generation, we propose the following three CNN stages: (1) a CNN for gender estimation, (2) a CNN for age-group estimation, and (3) a CNN for age regression. We conducted experiments using a large population gait database and confirm that the proposed method outperforms state-of-the-art benchmarks.

**Keywords:** Convolutional neural network, Age estimation, Gait feature

## 1 Introduction

Age estimation methods based on image processing have been extensively studied for various applications. Most of these studies focus on the images of faces, which tend to become more wrinkled and sag with age [1–6]. However, because high-resolution full-face images are required for these age estimation methods, they can only be used in situations where human images are captured at a short distance, e.g., age confirmation for purchasing alcohol and cigarettes or in digital signage applications.

In contrast, gait features, which represent a human's manner of walking, can be captured at a distance from an uncooperative subject. The way a human walks differs depending on his/her attributes, such as gender, physique, muscle mass, and age. From the medical view point, there are some studies on gait analysis to measure fatigue and detect disease [7, 8]. In the field of informatics, in contrast, gait-based human identification has been intensively studied for various applications such as access control, surveillance, and forensics [9–11]. Gait differs depending on not only attributes but also individuals. For instance, individual features greatly depend on posture, stride length, arm-swinging width, and the asymmetry of walking, which is formed from habits such as holding a shoulder bag on a fixed side. Moreover, gait identification has already been

used in practical cases in criminal investigations [12–14]. Hence, we expect that gait features will be useful for age information, and we investigated gait-based age estimation.

Gait-based age estimation expands the scope of real-world applications such as wide-area surveillance and the detection of lost children and wandering elderly people, as well as marketing research in large-scale facilities (e.g., shopping malls, terminals, and airports). There are several studies on gait-based age estimation. Makihara et al. [15] proposed an age regression algorithm based on Gaussian process regression (GPR). Lu et al. [16] proposed a multilabel-guided subspace to better characterize and correlate age and gender information, and Lu et al. [17] proposed an ordinary preserving manifold analysis (OPLDA) for gait-based age estimation. These methods unfold an image-based gait feature into a feature vector, where each dimension corresponds to each pixel. Because spatial proximity in the image structure is never considered, these methods can easily result in overtraining. To prevent this, we propose an age estimation approach using a convolutional neural network (CNN) that considers spatial proximity using a convolution operation and has had great success in many image recognition research areas.

Ideally, it is possible to achieve end-to-end learning by CNNs, i.e., any model can be trained by feeding raw images to the CNN. However, in practice, it is not easy to train networks in such an ideal situation. For this reason, existing researchers have proposed some designs in which pre-processed images are fed into the network instead of

\*Correspondence: [sakata@am.sanken.osaka-u.ac.jp](mailto:sakata@am.sanken.osaka-u.ac.jp)

<sup>†</sup>Atsuya Sakata and Noriko Takemura contributed equally to this work.

<sup>1</sup>The Institute of Scientific and Industrial Research, Osaka University, Ibaraki, Osaka, 5670047 Japan

Full list of author information is available at the end of the article

**Table 1** Layer configurations of *Single-CNN*

Layer	#Kernels	Size/stride	#Output nodes
conv1	81	$5 \times 5/1$	–
pool1	–	$3 \times 3/2$	–
conv1	45	$7 \times 7/1$	–
pool2	–	$2 \times 2/2$	–
fc3	–	–	1024
fc4_age	–	–	1

the raw images and constraints are added to the intermediate layers. In addition, recently, multi-task learning has attracted attention [18]: this method improves the accuracy of a target task by simultaneously learning target and other recognition tasks related to the target task. However, this method can instead worsen the accuracy of target tasks if other tasks adversely affect them because the model is trained to improve all the recognition tasks simultaneously.

Thus, in this paper, we propose sequential multi-task learning instead of conventional parallel multi-task learning. Each CNN for non-target tasks is trained one by one in sequence and the CNN for the target task is trained last. In this way, we can train the network to aim for the target task while taking other tasks into consideration.

Although the network architecture of sequential multi-task learning should be a deep CNN formed by chaining each CNN, we separately train each CNN, which has the same structure as those in parallel multi-task learning, in sequence to simply compare sequential with parallel multi-task by excluding the influence of the depth of the network. In other words, we predict a subject's gender and generation beforehand and then predict an age-by-age regression model trained on the data for each gender and generation combination separately.

We conducted a performance evaluation using the world's largest gait database, the OU-ISIR Gait Database, Large

Population Dataset with Age (*OULP-Age*) [19], which includes ages ranging from 2 to 90 years and males and females to confirm the effectiveness of the proposed method.

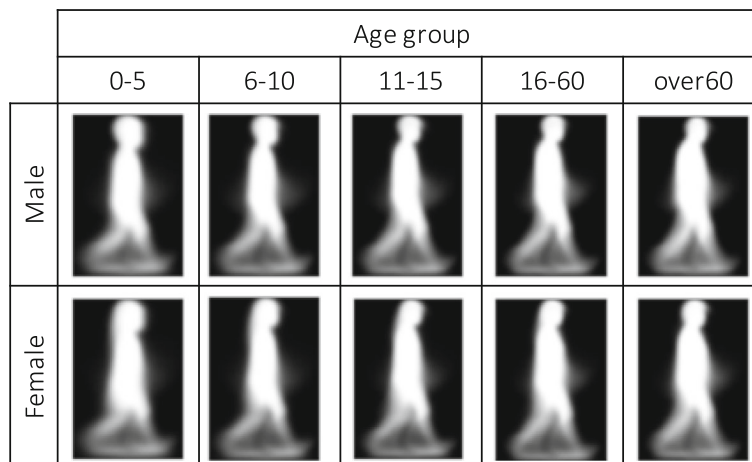
## 2 CNN-based age estimation

In this paper, the gait energy image (GEI) [20], which is a gait feature commonly used for gait-based person identification, is used as input to our CNNs. A GEI represents both dynamic features (i.e., swinging hands and legs while walking) and static features (i.e., human shapes and postures). We explain how to extract a GEI as follows. First, human silhouette sequences are obtained by background subtraction-based graph-cut segmentation. Second, we normalize silhouettes by size. Third, the gait period is detected from the normalized silhouette sequences, and finally, we generate a mean silhouette image based on the gait period.

### 2.1 Single CNN-based age estimation

Figure 2a shows the network structure for the CNN-based age estimator, and Table 1 shows the layer configurations. GEIs are fed into the CNN that contains two triplets of a convolution (conv) layer, batch normalization (norm) layer, and max pooling (pool) layer. It also consists of a pair of a fully connected (fc) layer and a norm layer, and a fc layer for recognition task. The conv layers and fc layers are followed by a ReLU activation function. We call a chain of layers from the input to norm3 in *Single-CNN* (a blue block shown in Fig. 2a) the *Conv block*.

We initialize the weight parameters of the CNN in all layers using He's method [21] and neuron biases with a constant of 0. We train our models using Adam with an initial learning rate of 0.001. We use dropout in the fc3 and fc4 layers with a probability of 0.8 and 0.5, respectively. The output of the final layer is considered to be the predicted age. We train the age estimator to minimize the

**Fig. 1** Mean GEIs for each gender and age group

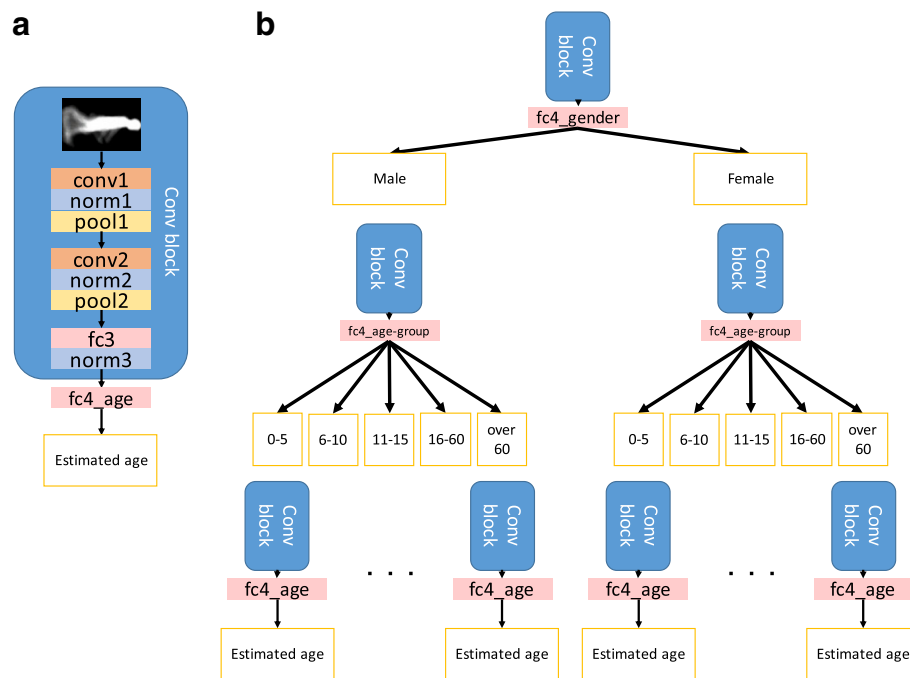


**Fig. 2** The architectures of (a) Single-CNN and (b) Sequential multi-CNN

mean absolute error (MAE) between the predicted and ground truth ages.

As mentioned in [9], in recognition tasks, variations in the input GEIs are smaller than those for a common object recognition task. Therefore, even such a shallow network can represent the feature of a subject's age.

## 2.2 Multistage CNN-based age estimation

Figure 1 shows the mean GEIs in the gait database (*OULP-Age*) for each gender and age group. It shows that gait features, e.g., human head-to-body ratio, hairstyles, shapes, and postures, vary depending on a subject's gender and generation.

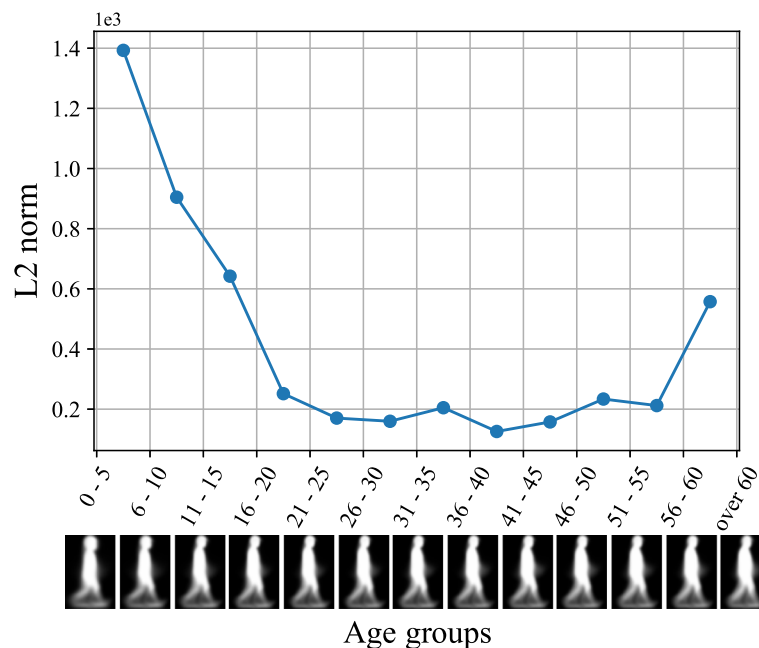


**Fig. 3** L2 distance between mean GEIs of adjacent age groups (*OULP-Age*). Silhouette images below the age-group labels represent mean GEl corresponding to each group

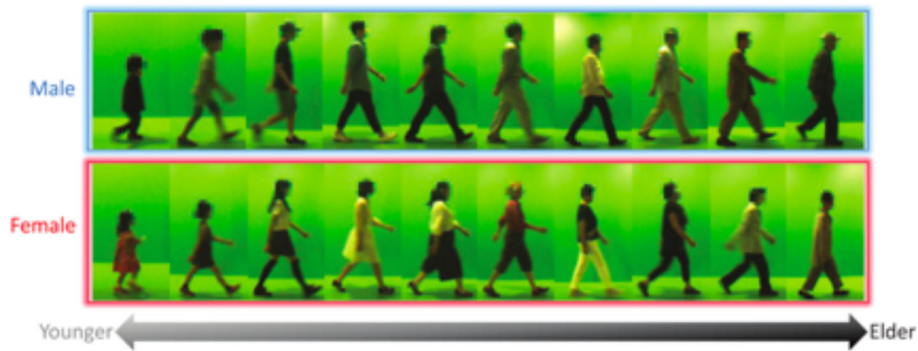


**Fig. 4** Data example in *OULP-Age* (cited from [19])

Thus, age estimation accuracy should improve in an age estimator based on specific genders and generations. In this paper, we attempt to improve age estimation using a multistage CNN composed of three CNN-based estimators, i.e., a gender estimator, age-group estimator, and age estimator (see Fig. 2b). Note the order of gender discrimination.

As shown in Fig. 2b, we used *Conv blocks* for all three estimators. For the gender estimator, the sigmoid normalized cross-entropy is employed as the loss function. For the age-group estimator, the number of outputs of the fc4 layer is changed to five (the number of age groups) and the softmax normalized cross-entropy is employed as a loss function.

### 2.2.1 Learning method

The learning procedure for multi-CNN age estimation (sequential multi-task CNN) is as follows (Fig. 2):

- 1 Train a gender estimator on a training set that includes all genders and all age groups
- 2 Predict gender by feeding the same training data set of (1) into the trained gender estimator
- 3 Train an age-group estimator for each predicted gender using the gender-predicted data from (2)
- 4 Predict the age group for each predicted gender by feeding the gender-predicted data from (2) into the trained age-group estimator for that gender
- 5 Train an age estimator for each predicted gender and each predicted age group using the data predicted in (4)

We train age estimators for each of the predicted gender and age-group estimators. Because of the decrease in the number of training data caused by this approach, overfitting can occur easily. To prevent this, we fine-tune pre-trained models. Specifically, the age-group estimator for each gender is trained by fine-tuning the age-group

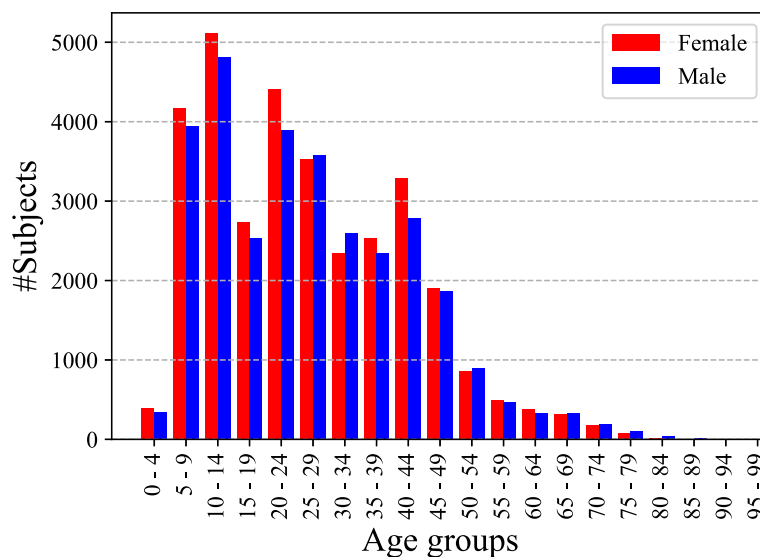


**Fig. 5** Distributions of subjects' age and gender in *OULP-Age*

estimator trained on all gender data, and the age estimator for each gender and each age group is trained by fine-tuning the age estimator trained on the all age-group data for each age.

### 2.2.2 Definition of age-group classes

We describe how we define age-group classes for the age-group estimator in multi-CNN age estimation. Gait data in *OULP-Age* are divided into several age groups based on GEI similarity.

First, we divided *OULP-Age* into intervals of 5 years and generated a mean GEI for each group. Note that samples over 60 years old were put into the same group because of a shortage of elderly persons' data. Second, we calculated the L2 distance between the mean GEIs of adjacent groups (Fig. 3). The L2 distance is calculated as

$$d_{L_2}(\mathbf{x}, \mathbf{y}) = \sqrt{\sum_{w=0}^{W-1} \sum_{h=0}^{H-1} \|x_{w,h} - y_{w,h}\|^2}, \quad (1)$$

where  $\mathbf{x}$  and  $\mathbf{y}$  are the mean GEIs of adjacent groups with height  $H$  and width  $W$ , respectively. Finally, we defined groups with an L2 distance that is less than a threshold as the same class and designed five classes: 0–5, 6–10, 11–15, 16–60, and over 60 years.

As we mentioned in Section 2, a GEI represents both dynamic features (i.e., swinging hands and legs while walking) and static features (i.e., human shapes and postures). Because people under 15 years old are growing swiftly, they change their static features substantially, and their GEIs have remarkable differences according to age. In contrast, as shown in Fig. 3, GEIs extracted from people who are between 15 to 60 years old almost do not appear to have changing features because they have almost stopped growing up. In other words, differences between static feature of GEI are more significant than those of dynamic feature. Poor accuracy during age-group estimation affects the next age regression stage, so we decided to split the age range into five age groups so that the CNNs can estimate age from the GEIs fairly precisely.

**Table 2** The number of subjects in the training set

Age group	Male	Female	Total
0–5	418	412	830
6–10	2349	2391	4740
11–15	2108	2265	4373
16–60	10,269	10,874	21,143
Over 60	452	385	837
Total	15,596	16,327	31,923

**Table 3** The number of subjects in the testing set

Age group	Male	Female	Total
0–5	405	425	830
6–10	2351	2389	4740
11–15	2119	2254	4373
16–60	10,220	10,923	21,143
Over 60	402	435	837
Total	15,497	16,426	31,923

## 3 Performance evaluation

### 3.1 Database

The OU-ISIR Gait Database, Large Population Dataset with Age (*OULP-Age*) [19] was used to evaluate the performance of the age estimation method. *OULP-Age* is the world's largest gait database that includes age and gender information. It consists of 63,846 gait images (31,093 males and 32,753 females) with ages ranging from 2 to 90 years. Figure 4 shows examples of the data, and Fig. 5 shows the distribution of subjects' age and gender in *OULP-Age*. Each subject walking from the right side to the left side along the walking course is captured by a USB camera set at a position 4 m away from the walking course. More information about the data capture is given in detail in [22]. GEIs of  $88 \times 128$  pixels extracted for a side-view gait are provided for each subject. We split the database into testing, training, and validation set at the ratio of 5:4:1, respectively. Note that 20% of the training set is used as the validation set. Tables 2 and 3 show the number of subjects among age groups and genders in the training set and testing set, respectively.

### 3.2 Training settings

The loss function for gender estimation and age-group estimation is cross entropy, which is calculated as

$$L(\mathbf{w}) = - \sum_{n=1}^N \sum_{m=1}^M t_{nm} \log y(I_n; \mathbf{w})_m, \quad (2)$$

where  $\mathbf{w}$  denotes the weight parameter matrix of the network,  $I_n$  is the input image,  $N$  is the number of data,  $M$  is the number of classes,  $y(I_n; \mathbf{w})_m$  is the  $m$ th element of the output vector, and  $t_{nm}$  denotes the ground truth class. The age estimation task is optimized by minimizing the mean absolute error between the ground truth and predicted age and is calculated as

**Table 4** Results for gender estimation with the training set

		Ground truth		Total
		Male	Female	
Predicted	Male	15,470	165	15,635
	Female	126	16,162	16,288
Total		15,596	16,327	31,923

**Table 5** Result for age-group estimator on the training set

		Ground truth					Total
		0-5	6-10	11-15	16-60	Over 60	
(a) Predicted as male							
Predicted	0-5	404	74	1	0	0	479
	6-10	10	2200	161	2	0	2373
	11-15	0	76	1459	77	5	1617
	16-60	0	7	485	10,120	119	10,731
	Over 60	0	0	3	73	359	435
Total		414	2357	2109	10,272	483	15,635
(b) Predicted as female							
Predicted	0-5	405	19	0	0	0	424
	6-10	11	2316	57	1	0	2385
	11-15	0	35	1919	83	0	2037
	16-60	0	13	288	10,776	40	11,117
	Over 60	0	0	0	11	314	325
Total		416	2,383	2,264	10,871	354	16,288

$$L(\mathbf{w}) = \frac{1}{N} \sum_{n=1}^N |t_n - y(I_n; \mathbf{w})|, \quad (3)$$

where  $\mathbf{w}$  denotes the weight parameter matrix of the network,  $I_n$  is the input image,  $N$  is the number of data,  $y(I_n; \mathbf{w})$  is the predicted age, and  $t_n$  is the ground truth age of the  $n$ th sample. For training each network included in the proposed method with back-propagation, we use Adam [23]. We also use a batch size of 128 samples, and the initial learning rate is 0.001, which is the default value for Adam. The maximum number of epochs is 100, although we used the weights of the network at the epoch when the validation error is the minimum. Table 4 shows the distribution among the gender, and Table 5 shows the distribution among the age groups.

**Table 6** MAEs and SDs for comparing the proposed methods with existing methods not based on CNNs

Method	MAE [years old]	SD [years old]
<i>Single-CNN</i>	6.22	6.52
<i>Sequential multi-CNN</i>	5.84	6.50
<i>GPR [15]</i>	7.30	6.64
<i>SVR [2]</i>	7.66	7.10
<i>OPLDA [17]</i>	8.45	7.04
<i>MLG [16]</i>	10.98	14.42

The best result is indicated by the italic font

### 3.3 Evaluation method

The MAE, standard deviation (SD), and cumulative score (CS) are used as the evaluation criteria for the performance evaluation. MAE is calculated as

$$\text{MAE} = \frac{1}{N} \sum_{n=1}^N |t_n - y_n|, \quad (4)$$

where  $t_n$  and  $y_n$  are the ground truth and predicted age values for the  $n$ th test sample, respectively, and  $N$  is the number of test samples. SD is calculated as follows.

$$\text{SD} = \sqrt{\frac{1}{N-1} \sum_{n=1}^N (|t_n - y_n| - \text{MAE})^2} \quad (5)$$

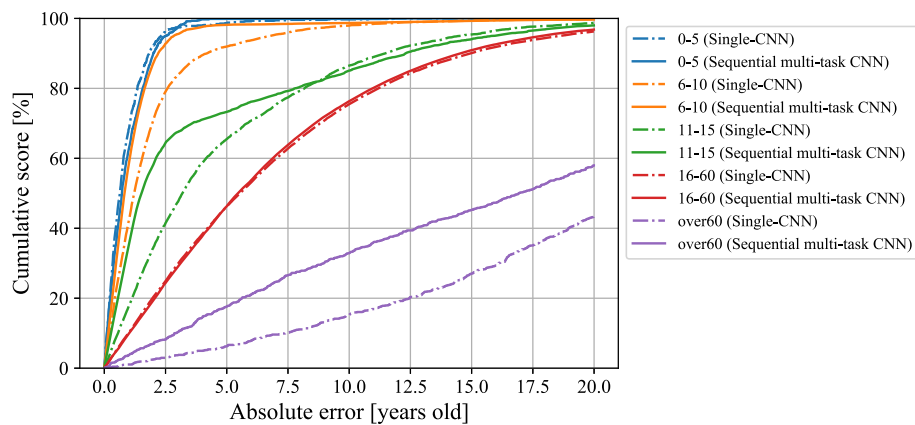
CS is calculated as

$$\text{CS}(l) = \frac{N_l}{N} \times 100\%, \quad (6)$$

where  $N_l$  is the number of samples whose MAE is within  $l$  year.

### 3.4 Comparison with existing methods not based on CNNs

We compared the two proposed methods with four comparison methods using the protocol described in [19].

**Fig. 6** Cumulative scores of *Single-CNN* and *Sequential multi-CNN*



**Table 7** MAEs and SDs for comparing the proposed method with a conventional multi-task CNN

Method	MAE [years old]	SD [years old]
<i>Sequential multi-CNN</i> (ours)	5.84	6.50
<i>Parallel multi-CNN</i>	6.23	6.61

The best result is indicated by the italic font

**Single-CNN** : Proposed method with a single CNN

**Sequential multi-CNN** : Proposed method with multiple CNN stages

**GPR** [15] : GPR-based method

**SVR** [2] : Support vector regression-based method

**OPLDA** [17] : OPLDA-based method

**MLG** [16] : A method that learns a multilabel-guided (MLG) subspace for human age

The MAEs and SDs of both versions of the proposed method and benchmarks are shown in Table 6. According to Table 6, the results of our CNN-based methods (*Single-CNN* and *Sequential multi-CNN*) are much better than those of the benchmarks. Furthermore, comparing the proposed methods, *Sequential multi-CNN*, which considers gender and age groups, improves the performance more than *Single-CNN*. In terms of SD, while the result of the proposed method is better than that of the existing method, there is no difference between our method and *Single-CNN*. This is because our method does not estimate age well for elderly people.

The CSs of *Single-CNN* and *Sequential multi-CNN* for each age group are shown in Fig. 6. As shown in the graph, *Sequential multi-CNN* significantly outperforms *Single-CNN*, especially in the 6–10, 11–15, and over 60 year groups.

### 3.5 Sequential multi-CNN vs. parallel multi-CNN

We compared the proposed method with multiple CNN stages (*Sequential multi-CNN*) with a conventional multi-

task CNN [24] (*Parallel multi-CNN*). In *Parallel multi-CNN*, multiple tasks are learned at the same time, while exploiting commonalities and differences across tasks to improve the estimation accuracy for the task-specific models. Figure 10 shows the network architecture of *Parallel multi-CNN*. Note that *Parallel multi-CNN* consists of the same *Conv block* with *Sequential multi-CNN* and each loss weight is 1.0, except that the last layer is branched for each task (gender, age group, and age), to compare only the learning strategy, namely, sequential multi-task learning vs. parallel multi-task learning.

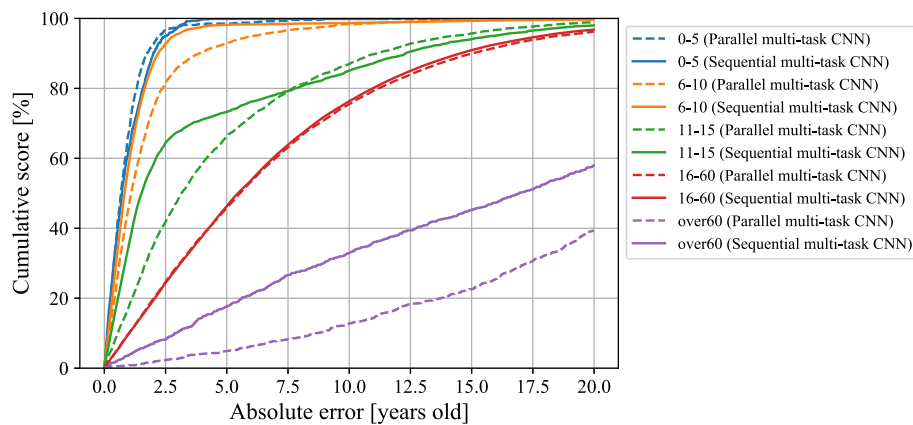
Table 7 shows the MAEs and SDs of *Sequential multi-CNN* and *Parallel multi-CNN* estimated in the same manner as in Section 3. The result of *Sequential multi-CNN* is better than that of *Parallel multi-CNN*. The CSs of *Parallel multi-CNN* and *Sequential multi-CNN* for each age group are shown in Fig. 7. The graph demonstrates that *Sequential multi-CNN* outperforms *Parallel multi-CNN*, as is the case for the comparison with *Single-CNN*.

In the training phase, *Sequential multi-CNN* is trained to minimize a loss for each task in the order of gender, age group, and age, i.e., the target task is the last one, whereas *Parallel multi-CNN* is trained so as to minimize multi-task losses simultaneously. Thus, *Sequential multi-CNN* can be trained more intensively and efficiently for the target task. This seems to be why the result of *Sequential multi-CNN* is better.

## 4 Discussion

### 4.1 Distribution of the estimated ages corresponding to the actual age

Figure 8 presents a scatter plot of the estimated ages of *Sequential multi-CNN* with respect to the ground truth age. Each point is colored according to the estimated age groups. According to Fig. 8, when age-group estimation fails, age estimation also fails, i.e., the MAE is larger, especially when the estimated age groups are 11–15 and over 60 years.

**Fig. 7** Cumulative scores of *Parallel multi-CNN* and *Sequential multi-CNN*

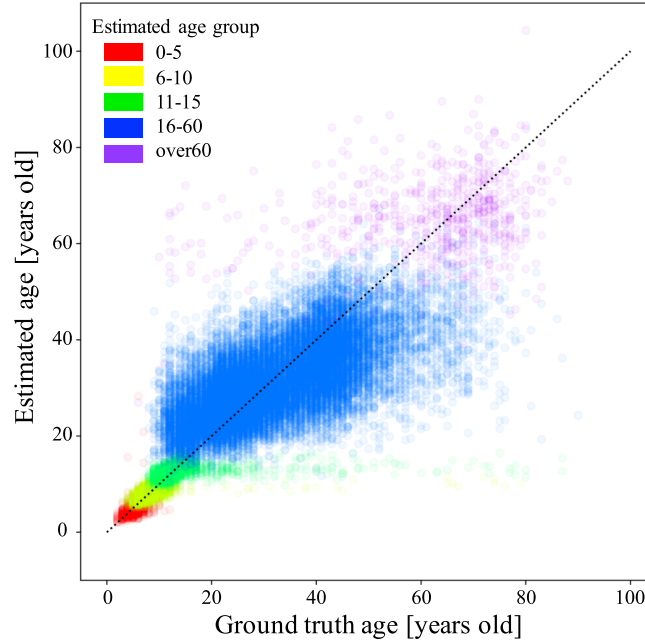


**Fig. 8** Scatter plot of the estimated ages of *Sequential multi-CNN* with respect to the ground truth age. The dotted line indicates where the estimated age equals the ground truth age

#### 4.2 Order of learning tasks in *Sequential multi-CNN*

In *Sequential multi-CNN*, CNNs are trained in the order of gender, age group, and age. The reasons why learning is performed in this order are as follows:

- Age is trained last because age estimation is the target task.
- Age group is trained second to the last because age group has a stronger relationship with age.
- Gender is trained first because gender is easier to recognize than age group.

Tables 8 and 9 show the confusion matrices of the results of gender and age-group estimation using the test set, respectively. These matrices show that the recognition rate of gender is higher than that of age group. More specifically, there are more than a few cases of incorrect recognition, especially for age-group estimation for pedestrians over 60 years. The proposed method has the problem that the failure of each estimation task causes successive failures in the next tasks. To avoid this, we need further studies to determine how to combine the CNNs at each stage into a single network so that it can effectively minimize the error of all the stages.

**Table 8** Results for gender estimation with the testing set

		Ground truth		Total
		Male	Female	
Predicted	Male	15,581	413	15,594
	Female	316	16,013	16,329
Total		15,497	16,426	31,923

#### 4.3 Difference of accuracy between male and female

Table 10 shows the gender-specific MAEs and SDs of *Sequential multi-CNN*, and Fig. 9 shows the graph of gender-specific CSs. As shown in Table 10 and Fig. 9, both MAE and SD of female subjects are worse than those of male subjects overall, especially over 60. Moreover, the CSs of *Sequential multi-CNN* is worse than that of *Single-CNN* in the case of 11–15 age group.

This is because the female-specific personal features such as hairstyle and clothes (e.g., skirt and one-piece)

**Table 9** Results for age-group estimation with the testing set

		Ground truth					Total
		0-5	6-10	11-15	16-60	Over 60	
(a) Male							
Predicted	0-5	266	212	1	1	0	480
	6-10	36	1912	350	4	9	2311
	11-15	0	213	1209	120	15	1557
	16-60	0	17	604	9969	244	10,834
	Over 60	0	0	9	137	266	412
Total		302	2354	2173	10,231	534	15,594
(b) Female							
Predicted	0-5	334	132	1	0	0	467
	6-10	108	2178	317	17	0	2620
	11-15	0	182	1099	271	3	1555
	16-60	0	66	756	10,367	257	11,446
	Over 60	0	2	5	81	153	241
Total		442	2560	2178	10,736	413	16,329



**Table 10** Gender-specific MAEs and SDs of *Sequential multi-CNN*

Gender	MAE [years old]	SD [years old]
Male	<i>5.60</i>	<i>6.19</i>
Female	<i>6.07</i>	<i>6.77</i>

The best result is indicated by the italic font

affect the accuracy of age estimation. It is easy to estimate age of both male and female children due to distinctive features such as height. Adult female, in contrast, have more variations in hairstyle and clothes than adult male. Therefore, it is more difficult to estimate the age of female than that of male in adult generation.

#### 4.4 Applicability of sequential multi-task learning to other tasks

In this paper, it was confirmed that sequential multi-task learning is more effective for age estimation than CNN-based single task learning and parallel multi-task learning (Fig. 10). The framework of sequential multi-task learning can be applied not only to age estimation but also to other recognition tasks, e.g., person identification and health estimation. Therefore, various applications of the

sequential multi-task learning can be expected in both the medical and information-science fields.

## 5 Conclusion

In this paper, we proposed a gait-based age estimation method using CNNs. To estimate ages based on differences in gait features depending on gender and generation, we proposed a method composed of three stages of CNNs: a gender estimator, an age-group estimator, and an age estimator. The results of the experiments using a large-scale gait database (*OULP-Age*) yielded an MAE of 5.84 years, which outperforms the benchmarks.

In the future, we plan to perform two studies to enhance age estimation. First, as mentioned in Section 4.2, we will train a deeper network formed by chaining CNNs for several tasks instead of a combination of sequential CNNs. In this way, we can avoid degrading the accuracy of the proposed method due to the incorrect recognition of each task. Second, we need to collect more gait data because the database we used lacks data on elderly subjects. By doing this, we will be able to improve our method for all generations.

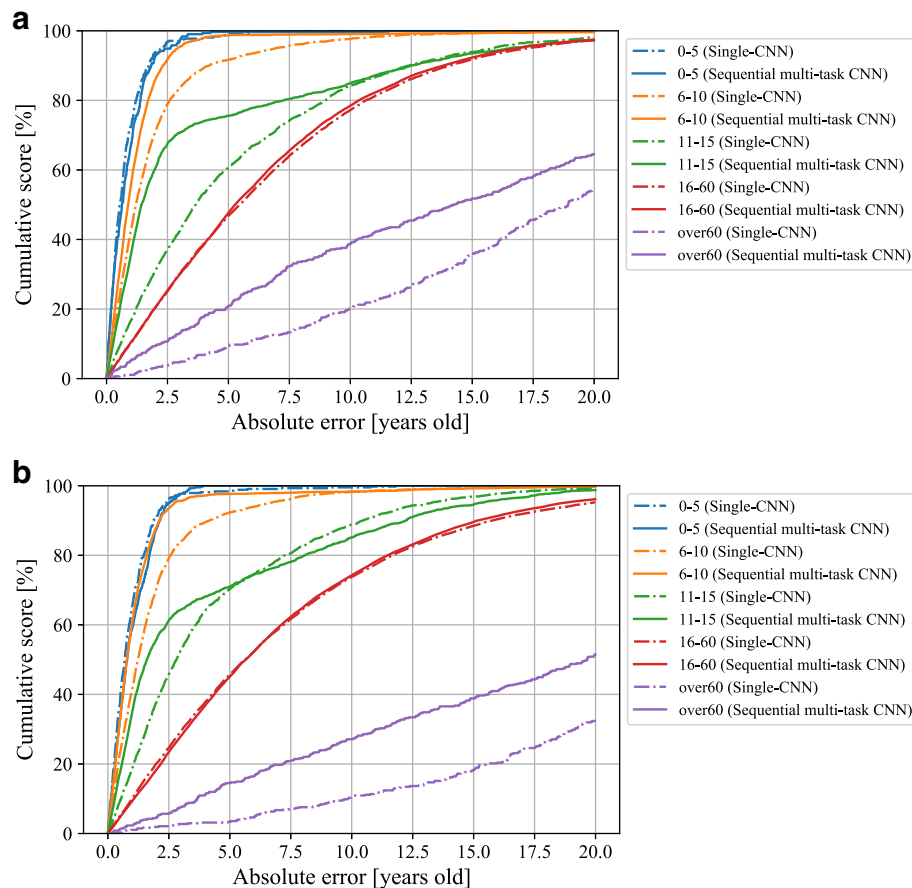
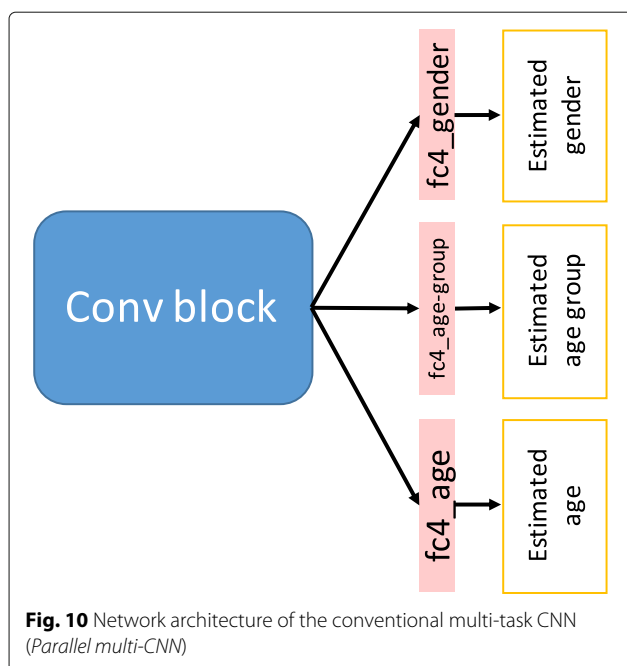


**Fig. 9** Gender-specific cumulative scores of *Sequential multi-CNN*. **a** Male. **b** Female



### Abbreviations

CNN: Convolutional neural network; CS: Cumulative score; GEI: Gait energy image; GPR: Gaussian process regression; MAE: Mean absolute error; MLG: Multilabel-guided subspace; OPLDA: Ordinary preserving manifold; OULP-Age: The OU-ISIR gait database, Large Population Dataset with Age

### Acknowledgements

Not applicable.

### Funding

This work was supported by JST-Mirai Program JPMJMI17DH.

### Availability of data and materials

The dataset supporting the conclusions of this article is available at <http://www.am.sanken.osaka-u.ac.jp/BiometricDB/index.html>.

### Authors' contributions

AS designed and executed the experiments and wrote the initial draft of the manuscript. NT contributed to the concept and helped to write the manuscript. YY supervised the work as well as gave technical support and conceptual advice. All authors reviewed and approved the final manuscript.

### Competing interests

The authors declare that they have no competing interests.

### Publisher's Note

Springer Nature remains neutral with regard to jurisdictional claims in published maps and institutional affiliations.

### Author details

<sup>1</sup>The Institute of Scientific and Industrial Research, Osaka University, Ibaraki, Osaka, 5670047 Japan. <sup>2</sup>The Institute for Datability Science, Osaka University, Suita, Osaka, 5650871 Japan.

Received: 18 November 2018 Accepted: 22 April 2019

Published online: 10 June 2019

### References

- Geng X, Yin C, Zhou ZH (2013) Facial age estimation by learning from label distributions. *IEEE Trans Pattern Anal Mach Intell* 35(10):2401–2412. <https://doi.org/10.1109/TPAMI.2013.51>
- Guo G, Fu Y, Dyer CR, Huang TS (2008) Image-based human age estimation by manifold learning and locally adjusted robust regression. *IEEE Trans Image Proc* 17(7):1178–1188. <https://doi.org/10.1109/TIP.2008.924280>
- Fu Y, Huang TS (2008) Human age estimation with regression on discriminative aging manifold. *IEEE Trans Multimed* 10(4):578–584. <https://doi.org/10.1109/TMM.2008.921847>
- Zhang YZY, Yeung D-YYD-Y (2010) Multi-task warped Gaussian process for personalized age estimation. 2010 IEEE Conf Comput Vis Pattern Recog (CVPR):2622–2629. <https://doi.org/10.1109/CVPR.2010.5539975>
- Niu Z, Zhou M, Wang L, Gao X, Hua G (2016) Ordinal regression with multiple output CNN for age estimation. 2016 IEEE Conf Comput Vis Pattern Recog (CVPR):4920–4928. <https://doi.org/10.1109/CVPR.2016.532>
- Escalera S, Fabian J, Pardo P, Baro X, Gonzalez J, Escalante HJ, Misevic D, Steiner U, Guyon I (2015) ChaLearn looking at people 2015: apparent age and cultural event recognition datasets and results. *Proc IEEE Int Conf Comput Vis* 2015-Febru:243–251. <https://doi.org/10.1109/ICCVW.2015.40>
- Janssen D, Schöllhorn WJ, Newell KM, Jäger JM, Rost F, Vehof K (2011) Diagnosing fatigue in gait patterns by support vector machines and self-organizing maps. *Hum Mov Sci* 30(5):966–975. <https://doi.org/10.1016/j.humov.2010.08.010>. EWOMS 2009: The European Workshop on Movement Science
- Liao R, Makihara Y, Muramatsu D, Mitsugami I, Yagi Y, Yoshiyama K, Kazui H, Takeda M (2014) Video-based gait analysis in cerebrospinal fluid tap test for idiopathic normal pressure hydrocephalus patients (in Japanese). In: The 15th Annual Meeting of the Japanese Society of NPH, Suita, Japan
- Takemura N, Makihara Y, Muramatsu D, Echigo T, Yagi Y (2017) On input/output architectures for convolutional neural network-based cross-view gait recognition. *IEEE Trans Circ Syst Video Technol* PP(99):1–1. <https://doi.org/10.1109/TCSVT.2017.2760835>
- Wu Z, Huang Y, Wang L, Wang X, Tan T (2017) A comprehensive study on cross-view gait based human identification with deep CNNs. *IEEE Trans Pattern Anal Mach Intell* 39(2):209–226. <https://doi.org/10.1109/TPAMI.2016.2545669>
- Makihara YS, Matovski DS, Nixon MN, Carter J, Yagi Y (2015) Gait recognition: databases, representations, and applications. In: Webster JG, editor. *Wiley Encyclopedia of Electrical and Electronics Engineering*. <https://doi.org/10.1002/047134608X.W8261>
- Bouchrika I, Goffredo M, Carter J, Nixon M (2011) On using gait in forensic biometrics. *J Forensic Sci* 56(4):882–889. <https://doi.org/10.1111/j.1556-4029.2011.01793.x>
- Lynnerup N, Larsen PK (2014) Gait as evidence. *IET Biom* 3:47–547
- Iwama H, Muramatsu D, Makihara Y, Yagi Y (2013) Gait verification system for criminal investigation. *Inf Media Technol* 8(4):1187–1199. <https://doi.org/10.1185/imt.8.1187>
- Makihara Y, Okumura M, Iwama H, Yagi Y (2011) Gait-based age estimation using a whole-generation gait database. In: 2011 International Joint Conference on Biometrics, IJCB 2011. <https://doi.org/10.1109/IJCB.2011.6117531>
- Lu J, Tan YP (2010) Gait-based human age estimation. *IEEE Trans Inf Forensics Secur* 5(4):761–770. <https://doi.org/10.1109/TIFS.2010.2069560>
- Lu J, Tan YP (2013) Ordinary preserving manifold analysis for human age and head pose estimation. *IEEE Trans Hum-Mach Syst* 43(2):249–258. <https://doi.org/10.1109/TSMCC.2012.2192727>
- Caruana R (1997) Multitask learning. *Mach Learn* 28(1):41–75. <https://doi.org/10.1023/A:1007379606734>
- Xu C, Makihara Y, Ogi G, Li X, Yagi Y, Lu J (2017) The OU-ISIR Gait Database comprising the Large Population Dataset with age and performance evaluation of age estimation. *IPSJ Trans. Comput Vis Appl* 9:1–14. <https://doi.org/10.1109/TIFS.2012.2204253>
- Han J, Bhanu B (2006) Individual recognition using gait energy image. *IEEE Trans Pattern Anal Mach Intell* 28(2):316–322. <https://doi.org/10.1109/TPAMI.2006.38>. arXiv:1307.5748v1
- He K, Zhang X, Ren S, Sun J (2015) Delving deep into rectifiers: surpassing human-level performance on imagenet classification. *CoRR* abs/1502.01852. [1502.01852](https://arxiv.org/abs/1502.01852)
- Makihara Y, Kimura T, Okura F, Mitsugami I, Niwa M, Aoki C, Suzuki A, Muramatsu D, Yagi Y (2016) Gait collector: an automatic gait data collection system in conjunction with an experience-based long-run exhibition. In: 2016 International Conference on Biometrics (ICB). pp 1–8. <https://doi.org/10.1109/ICB.2016.7550090>
- Kingma DP, Ba J (2014) Adam: a method for stochastic optimization. pp 1–15. <https://doi.org/10.1145/1830483.1830503>. [1412.6980](https://arxiv.org/abs/1412.6980)
- Marín-Jiménez MJ, Castro FM, Guil N, de la Torre F, Medina-Carnicer R (2017) Deep multi-task learning for gait-based biometrics. In: 2017 IEEE International Conference on Image Processing (ICIP). pp 106–110. <https://doi.org/10.1109/ICIP.2017.8296252>